Fully Automated Attractor Analysis of Cyanobacteria Models

Nikola Beneš, Luboš Brim, Samuel Pastva, David Šafránek, Matej Troják
Faculty of Informatics
Masaryk University
Brno, Czech Republic
{xbenes3, brim, xpastva, safranek, xtrojak}@fi.muni.cz

Jan Červený, Jakub Šalagovič
Global Change Research Institute
Czech Academy of Sciences
Brno, Czech Republic
cerveny.j@czechglobe.cz

***Abstract*—Complex dynamics arising in biological systems can be characterised by various kinds of attractors. To that end, the task of determining attractors becomes important in modern systems analysis. Biological systems are typically formalised as highly parametrised continuous-time ODE models. Such models can be abstracted in the form of parametrised graphs. In such abstractions, attractors are observed in the form of terminal strongly connected components (tSCCs). In this paper, we demonstrate a novel method for detecting tSCCs in parametrised graphs on several models of cyanobacteria taken from the domain-specific online platform e-cyanobacterium.org.**

***Index Terms*—attractors, parametrised graph, terminal strongly connected components, cyanobacteria**

I. Introduction

Molecular interactions in biological systems form complex structures of negative or positive feedbacks. The interplay of such interactions can emerge in behaviour that is hard to predict. Systems behaviour in long time horizon may be significantly affected by concurrent flows of complex information. Some of the problems related to the study of systems dynamics can be significantly simplified if we concentrate on the *long-term behaviour*. This idea finds its mathematical expression in the concept of an *attractor*.

In general, attractors are of strong interest as they concentrate system states to which the dynamics converges or resides there forever once reached. To that end, *stable attractors* are important as they typically represent robust modes of system' dynamics. Several analysis techniques frequently used in systems biology investigate a system in a stable attractor. A typical example is flux balance analysis.

In general, an important problem of systems analysis is to determine the number and position of attractors. Biological systems are usually described by models represented as highly parametrised differential equations (ODEs). Owing to the non-linear character of these equations, dynamics of these models is markedly sensitive to changes in parameters.

Methods that fully automatise analysis of attractors for a given parameterisation are needed to ensure that models are set and used correctly. Moreover, it is important to know how attractors and their character change with parameters. This allows not only to identify parameter ranges where a system behaves as expected in long-time horizon, but also to investigate critical parameter values where the expected long-time behaviour can be violated (e.g., the system changes the number or shape of its attractors).

In [1] we have introduced a method that fully automatises the analysis of attractors with respect to uncertain parameters. The method utilises computer scientific techniques – formal methods and graph algorithms – to identify attractors in non-linear ODE models. In contrast to numerical (or analytic-numerical) methods that work locally in terms of requiring to know the approximate position of the attractor [2], our approach works fully in the global scope. This is achieved by computing over discrete abstractions of continuous dynamics [3]–[5]. In the discrete setting, the problem is reduced to identification of strongly connected components (SCCs) in the graph (state-transition system) that over-approximates the continuous systems dynamics [6]. It is worth noting that identification of SCCs can be done efficiently for higher-dimensional systems in the non-parametrised case [7]–[9]. However, in case of biological models, parameters are often not completely known. Moreover, the parameter space explodes combinatorially with the arity of component influences causing parameter uncertainty to result in enormously large sets of parameter values. To that end, our approach provides a heuristics and parallelisation that scale well with the number of uncertain parameters.

In this paper, we present a case study of our algorithms performed on several ODE models describing dynamics of processes in cyanobacteria. To that end, we have selected models implemented online on the e-cyanobacterium.org platform [10]. E-cyanobacterium is a long-term project that aims at the model-based and experimental investigation of biophysical processes occurring in cyanobacteria. The crucial part of the platform is model repository that provides a database of ODE models developed by experts on cyanobacteria biophysics. Automatised analysis of the models is the part of online services offered by e-cyanobacterium.org. The focus is given to simulation of model dynamics with respect to user-defined parameters. It is highly important to provide users parameter ranges where models behave correctly. Automated detection of attractors and computing parameter values for which they

This work has been supported by the Czech Science Foundation grant 18-00178S and by the Czech National Infrastructure grant LM2015055.

are present in the system thus makes one of the important tasks making a part of the curation procedure of the systems models implemented in the platform.

II. Methods

The method as described in [1] assumes a parametrised directed graph $G = (V, E, \mathbb{P})$. Here, $\mathbb{P}$ represents the set of all possible parameter valuations and each edge is augmented with a set of parameter valuations which enables it, $E \subseteq V \times \mathbb{P} \times V$. In this section, we first show how this parametrised graph is constructed from a set of continuous differential equations and then discuss how such graph can be used to reason about attractors in the original system.

The process starts with a non-linear ODE model. This model is transformed into a piece-wise multi-affine approximation which can be safely over-approximated by a rectangular abstraction procedure. The result is a parametrised graph that is searched using a divide-and-conquer algorithm in order to obtain all terminal strongly connected components (tSCCs). Such components then over-approximate the attractors in the piece-wise multi-affine system.

Model. We consider $\mathbb{P} \subseteq \mathbb{R}^m$ to be a *bounded continuous parameter valuation space* of dimension m. A *biological ODE model* $\mathcal{M}$ is given as a system of autonomous ordinary differential equations of the form $\dot{x} = f(x, \mu)$. Here, $x = (x_1, \ldots, x_n) \in \mathbb{R}^n$ is a vector of variables, $\mu = (\mu_1, \ldots, \mu_m)$ is a vector of parameters such that μ is evaluated in $\mathbb{P}$, $f = (f_1, \ldots, f_n)$ is a vector of derivation functions $\mathbb{R}^n \times \mathbb{R}^m \to \mathbb{R}$, and we require each f_i to be affine in μ. Finally, we assume each variable x_i is bounded within an interval $[x_i^{min}, x_i^{max}]$ and that no trajectory exits this interval, formally $\forall p \in \mathbb{P}, \forall i \in \{1, \ldots, n\} : (x_i = x_i^{min} \Rightarrow f_i(x, p) > 0) \wedge (x_i = x_i^{max} \Rightarrow f_i(x, p) < 0)$.

Since these restrictions allow f to be non-linear in x, they are satisfied by the majority of available models with appropriate bounds. This includes models representing variants of enzyme or Hill kinetics where parameters are independent and do not appear in an exponent or a denominator of a kinetic function.

Approximation. To proceed with the discretisation, the model $\dot{x} = f(x, \mu)$ has to satisfy the criterion that every f_i is piecewise multi-affine (PMA) in x. To transform the model into this form, we employ the approach defined in [5]. In particular, each non-linear member in f_i is approximated with an optimal sequence of piece-wise affine ramp functions. During this procedure, a finite number of thresholds is introduced for every component of x.

The crucial factor of the approximation error is the number of piece-wise affine segments. Though there is not yet a method that would somehow propagate the information on approximation error into the trajectories of the resulting PMA model, it has been shown on several case studies that sufficiently fine approximation does affect the system's vector field only negligibly [5], [10].

Abstraction. We employ the rectangular abstraction [3], [5] in order to transform a piece-wise multi-affine ODE model into a discrete parametrised graph. For each variable x_i, we assume a set of thresholds $\theta_i^1 < \theta_i^2 < \ldots < \theta_i^{n_i - 1} < \theta_i^{n_i}$ such that $\theta_i^1 = x_i^{min}$ and $\theta_i^{n_i} = x_i^{max}$ (these typically come from the approximation procedure, but can be also introduced by the user). This set of thresholds partitions the admissible space into n-dimensional intervals called rectangles. Each rectangle is uniquely represented by an n-tuple $R(j_1, \ldots, j_n) = [\theta_1^{j_1}, \theta_1^{j_1+1}] \times \ldots \times [\theta_n^{j_n}, \theta_n^{j_n+1}]$ where each $j_i \in \{1, \ldots, n_i - 1\}$. We also define $VR(j_1, \ldots, j_n)$ to be the set of all vertices of $R(j_1, \ldots, j_n)$. Finally, in every rectangle, we expect each f_i to be multi-affine in x and affine in μ.

The abstraction results in a symbolic description of a parametrised graph, $G = (V, E, \mathbb{P})$ where $V = \{(j_1, \ldots, j_n) \mid j_i \in \{1, \ldots, n_i - 1\}\}$ such that each $v \in V$ represents one rectangle $R(v)$. We then say that $u \in V$ *is above* $v \in V$ *in dimension* i if $u_i = v_i + 1$ and for all $j \neq i$, $u_j = v_j$. Symmetrically, u *is below* v *in dimension* i if $u_i = v_i - 1$ and for all $j \neq i$, $u_j = v_j$.

An edge $u \xrightarrow{p} v$ is then created for each $p \in \mathbb{P}$ such that

- u is *above* v in dimension i and there exists $\hat{x} \in VR(u) \cap VR(v)$ such that $f_i(\hat{x}, p) < 0$;
- u is *below* v in dimension i and there exists $\hat{x} \in VR(u) \cap VR(v)$ such that $f_i(\hat{x}, p) > 0$.

Additionally, there is a self-loop defined for any $u \in V$ and $p \in \mathbb{P}$ such that $\forall p \in P : \mathbf{0} \in \{f(\hat{x}, p) | \hat{x} \in hull(VR(u))\}$.

A subset $P \subseteq \mathbb{P}$ of parameter values is associated with every edge denoting the situations under which the corresponding transition is enabled. Finite number of thresholds implies finite number of distinct parameter sets that can appear on transitions in the model. In consequence, total number of parameter sets for an abstraction of model $\mathcal{M}$, denoted $|\mathbb{P}_{|\mathcal{M}}|$, is finite.

The existence of a fixed point in a system can be approximated by the rectangular abstraction. This is achieved conservatively by introducing a self-edge for every rectangle such that there is a zero vector included in the convex hull of all vertices of the rectangle. This is a necessary condition for the existence of a point where the derivatives in all coordinates are zero. Under this setting, it has been shown that rectangular abstraction is conservative (overapproximation) with respect to almost all trajectories of the approximated (PMA) model [11].

The conservativeness of the abstraction together with the consideration of only those parameter values for which the dynamics are bounded imply that *every tSCCs in the abstraction must cover at least one attractor in the PMA system*. This also implies that the number of discovered tSCCs in the abstraction is a lower bound for the number of attractors in the corresponding PMA system and that their location is over-approximated by the location of the tSCCs. While this allows us to bound the attractor in a specific region of the state space, it does not provide information about the analytical nature of the attractor (equilibrium, limit cycle, chaotic attractor, etc.).

Component search.

Once a parametrised graph is constructed, it can be investigated using our parallel tSCC detection algorithm proposed in [1]. The algorithm works by selecting a pivot vertex u

and dividing the vertices of the graph into three subsets: The first set contains tSCCs reachable from u, the second set contains tSCCs not reachable from u, and the third set contains vertices which do not belong into any tSCC. The algorithm then recursively proceeds in first two sets until pivot itself belongs into a tSCC.

The efficiency of this procedure relies on a combination of symbolic and parallel approach. The parameter valuation sets are represented symbolically, providing a compact representation of the parameter space while the sets of rectangle vertices remain explicit, allowing parallel and even distributed computation. Implementation is now available in the tool Pithya [12].

III. E-cyanobacterium Platform

E-cyanobacterium [13] is a framework serving for analysis, visualisation, annotation, and public sharing of mathematical models and biological experiments concerning the biochemistry of cyanobacteria. The framework integrates abstract dynamical models with *Biochemical Space* (BCS) – a detailed rule-based biochemical description. The framework includes several modules that foster the presentation and creation of the models. The general goal is to connect biological knowledge with the profits of computational systems biology tools.

Model Repository makes a crucial part of the platform. It is represented by a database of the models describing biological processes. Reaction network of each model is transformed into a set of ordinary differential equations (ODEs). To represent multiple biological scenarios and to enable analyses with particular settings, the model is associated with *data sets* (parameter values).

The model reaction network is composed by a set of components and a set of reactions. Every reaction describes interactions of a subset of specified components with a given reaction rate. For better scalability and usability, the rate can be specified as a mathematical expression using a predefined set of parameter constants or assignments. An important part of the model is annotation which increases its reliability and information gain.

It is possible to change initial conditions and parameter constants of the model and set the simulation options (the numerical solver, simulation time, etc.) in a so-called *data set*. The simulations can be run online and the time-series plot is generated for all available datasets. In the plot, it is possible to alter the type of the axes, select particular curves, zoom, and display a value on a curve. Simulation data export is equipped by multiple data formats.

Additionally, static analysis implements the following three tasks: *modes analysis* producing elementary flux modes, *conservation analysis* producing mass conservation analysis (moiety conservation), and *matrix analysis* producing stoichiometry matrix. For all the tasks, the well-acclaimed third-party tool COPASI [14] is used to enable downloading the results in an SBRML file [15].

Models are integrated within BCS which ensures that all parts of the model are enriched by the biological annotation. This can help to interlink models by overlapping parts among them. Additionally, a model can also be related to a wet-lab experiment which can support relevance and credibility of the model.

In the following sections, we briefly describe four non-linear models from the repository which will be analysed using techniques described in Section II.

Clark model [16] describes the fluxes of inorganic carbon from cytosol to carboxysome of cyanobacteria and its fixation using carbonic anhydrase and *RuBisCO* enzyme.

Carbon dioxide concentrating mechanism (CCM) of cyanobacteria consists of structural enzymes and proteins that enable the increase of the local concentration of CO_2 around the carbon-fixing enzyme *RuBisCO* (ribulose-1,5-bisphosphate carboxylase/oxygenase) up to three orders of magnitude. Cyanobacterial growth in a native aqueous environment with low concentrations of CO_2 is enabled by the mechanism. The mechanism is described by the model and it is shown that the CCM is not necessary for growth in media in equilibrium with concentration of 10% CO_2 (which is available in industrial flue gas). Since the proteins involved in the CCM are quite large (i.e. costly to synthesise), the elimination of their production in an environment with high-CO_2 concentration could provide an important metabolic benefit to cyanobacteria.

The model has four variables: CO_2_cyt (carbon dioxide in cytosol) in the range $[0, 0.0001]$, HCO_3_cyt (hydrogencarbonate in cytosol) in the range $[0, 0.1]$, CO_2_carb (carbon dioxide in carboxysome) in the range $[0, 0.001]$, and HCO_3_carb (hydrogencarbonate in carboxysome) in the range $[0, 0.1]$. Moreover, there is a parameter $fast$ which affects rate of carbon fixation reaction[1] in the range $[1,\ 500]\ h^{-1}$ (from very slow to very fast).

All variables had 40 thresholds, which produced the state space of size approximately 2.5×10^6 discrete states.

Grimaud model [17] describes the time-dependent dynamics of diazotrophy in a unicellular cyanobacterium, *Crocosphaera watsonii WH8501*, with respect to obligate diazotrophy and light limitation.

The model is divided to into several pools. An intercellular pool describes the nitrogenase enzyme. An intracellular nitrogen and carbon are both divided into a storage and a functional pool. A very complex dynamics of the model are driven by the light regime and the various intracellular nitrogen and carbon flow between these pools. The model dynamics are validated with cultures experiments of *C. watsonii* under different light regimes, showing that the proposed mechanisms reproduce the growth dynamics of this organism. The model demonstrates how nitrogen and carbon are coupled along with nitrogenase activity constrained by the light regime.

The model has four variables: C_{nit} (nitrogenase pool) in range $[0, 1]$, N_r (nitrogen storage pool) in the range $[0, 200]$, C_r (carbohydrates pool) in the range $[0, 400]$, and C_f (functional carbon pool) in the range $[0.001, 1000]$; and three

[1]Carbon fixation is the conversion process of inorganic carbon (carbon dioxide) to organic compounds by living organisms.

assignments C_{tot} (total carbon of *C. watsonii*), N_{tot} (total nitrogen of *C. watsonii*), and N_f (functional nitrogen pool), with meaning of sums of some of the variables. Additionally, there is a parameter r_2 expressing the maximum carbon fixation rate considered in the range $[0.09,\ 0.825]\ h^{-1}$ and parameter r_4 expressing nitrogenase synthesis rate allowed in the range $[0.00031,\ 0.00279]\ h^{-1}$.

Finally, since the model is not autonomous, we consider time as an additional variable with the derivative set to 1 and bound by an interval of $[0, 200]$. This is a reasonable approach since the model itself behaves periodically (with a period of 24 time units), hence this gives us an over-approximation of the attractor after a little more than 8 time periods.

All variables had 10 thresholds except C_f with 40 thresholds and time with 20. Together it produced the state space of size approximately 5.5×10^5 discrete states.

Müller model is a prototype version of the dynamical model of carbon fluxes in a laboratory scale photobioreactor (e.g. intercellular exchange, carbonate chemistry, and gas-to-liquid CO_2 transfer).

To identify maximum production rates of biofuels or biomass and to reason about the cellular mechanisms of carbon fixation, all CO_2 related exchange rates of a photosynthetic culture can be estimated by the model. The model aspires to become a part of a project for the design of upscaled bioreactors to industrial level.

The model consists of seven variables: OH^- (hydroxide) in the range $[0, 1]$, H^+ (proton) in the range $[0, 1]$, CO_3^{2-} (carbonate) in the range $[0, 50]$, HCO_3^- (hydrogencarbonate) in the range $[0,\ 3000]$, CO_2 (carbon dioxide) in the range $[0, 150]$, HA (Brønsted acid) in the range $[7000, 10000]$, and A (Brønsted base) in the range $[0, 7000]$. There is a parameter $kLa\_CO_2\_eff$ expressing volumetric mass transfer coefficient from gas headspace to medium allowed in the range $[10,\ 200]$.

All variables had 10 thresholds, which produced the state space of size approximately $4.7 \cdot 10^6$ discrete states.

Plyusnina model is an incomplete model of electron transport on thylakoid membrane of cyanobacteria. The model is unfinished, yet exhibits interesting properties suitable for demonstration of our analysis methods.

The specific feature of electron transport on thylakoid membrane of cyanobacteria is a combination of photosynthetic and respiratory pathways in one reaction space, connected through plastoquinone pool (PQ). To couple the electron transfer in thylakoid membrane with metabolic reactions of central metabolism, the model considers influx and outflux of $NAD(P)H$ and ATP in cytoplasm in simple form. For every complex redox reaction two abstract states are used – a more oxidized (with index 'o') and a more reduced (with index 'r'). Although such consideration is rather rough, it allows to represent electron pathways in the most simple form and to reflect the main features and stoichiometry of redox reactions.

The model consists of eight variables: H_i and H_o (different types of proton) both in range $[0, 10]$, ATP (adenosine triphosphate) in the range $[0, 1]$, $NADH$ (nicotinamide adenine dinucleotide) in the range $[0, 1]$, $NADPH$ (dihydronicotinamide-adenine dinucleotide phosphate) in the range $[0, 1]$, $pqh2$ (plastoquinol) in range $[0, 1]$, fd (ferredoxin) in the range $[0, 2]$, and pc (plastocyanin) in the range $[0, 2]$. There are no unknown parameters considered in the model.

All variables had 8 thresholds, which produced the state space of size approximately $5.7 \cdot 10^6$ discrete states.

IV. Results

The results of Terminal Component Detection analysis for all of the models from Section III are described subsequently in the following paragraphs. Since the amount of computed data is extremely large and multi-dimensional, we provide several manually obtained visualisations of the most interesting findings. The complete data are available for download[2].

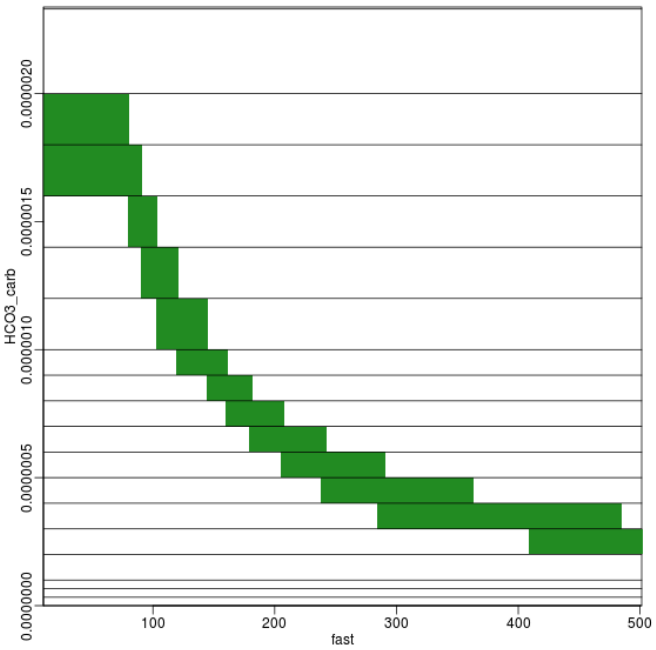

Fig. 1. Visual representation of the dependence of variable HCO_3_carb on the value of parameter $fast$ in the Clark model. The attractor (green) is changing with the value of the parameter.

Clark model. The analysis has shown there is a single attractor. Fig. 1 shows the attractor level of $HCO3\_carb$ with respect to the changes of the parameter $fast$ representing carbon fixation rate. The result is in agreement with the expected system behaviour because $fast$ has a crucial impact on the system dynamics. In particular, the interpretation is that the concentration of HCO_3 kept in carboxysome decreases with the parameter. This correlates with behaviour of CO_2, as shown in Fig. 2 – the long time CO_2 carbon form residing in carboxysome increases with $fast$.

The full dimensional attractor is enclosed within the following rectangular region: $CO_2\_cyt[8 \times 10^{-6}, 10^{-5}] \times HCO_3\_cyt[6 \times 10^{-7}, 2 \times 10^{-5}] \times CO_2\_carb[2 \times 10^{-6}, 10^{-3}] \times$

[2]http://biodivine.fi.muni.cz/paper/ICSTCC2018/results.zip

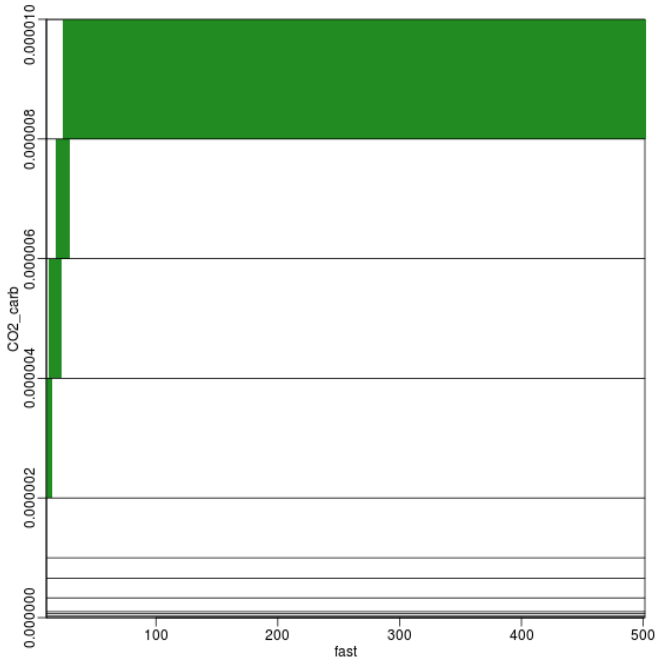

Fig. 2. Visual representation of the dependence of variable HCO_3_cyt on the value of parameter *fast* in the Clark model. The attractor (green) is changing with the value of the parameter.

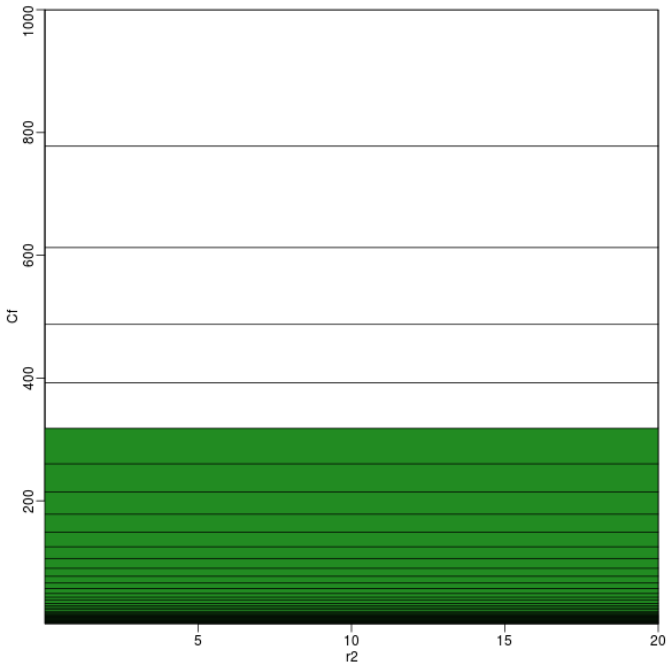

Fig. 3. Visual representation of the independence of variable C_f (functional carbon pool) on the value of parameter r_2 (carbon fixation rate) in the Grimaud model. The attractor (green) remains the same regardless of the value of the parameter.

$HCO_3\_carb[3 \times 10^{-8}, 2 \times 10^{-6}]$. However, the computed results have shown that the actual shape of the attractor does not fill the entire volume of this region. In particular, it covers approximately 8% of the volume of this region.

Grimaud model. The analysis has shown there is a single attractor. As expected, the attractor resides in the last considered time interval, since the time is monotonous. An interesting fact is that the attractor is independent on both considered parameters (for example, see Fig. 3). It is in contrast with the case of the Clark model which showed an intense dependence on the respective parameter. However, the models cannot be directly compared due to the different levels of abstraction and different modelling approaches (the Grimaud model describes the whole carbon and nitrogen pools instead of individual chemical objects).

The size of the model makes the visualisation of the attractor in two dimensional space almost impossible. The attractor is enclosed in the following rectangular region: $C_{nit}[0, 0.1] \times N_r[0, 88.8] \times C_r[0, 44.4] \times C_f[10^{-3}, 318.32]$ and the shape of the attractor is very regular, thus its volume is practically equal to the volume of the rectangular region. Additionally, a slice of the attractor state space is presented in Fig. 4.

Müller model. The analysis has shown there is a single attractor. Additionally, the analysis has shown that the parameter $kLa\_CO_2\_eff$ expressing volumetric mass transfer coefficient from gas headspace to medium has no influence on the attractor position and shape (see Fig. 5 for the two-dimensional projection of the computed attractor).

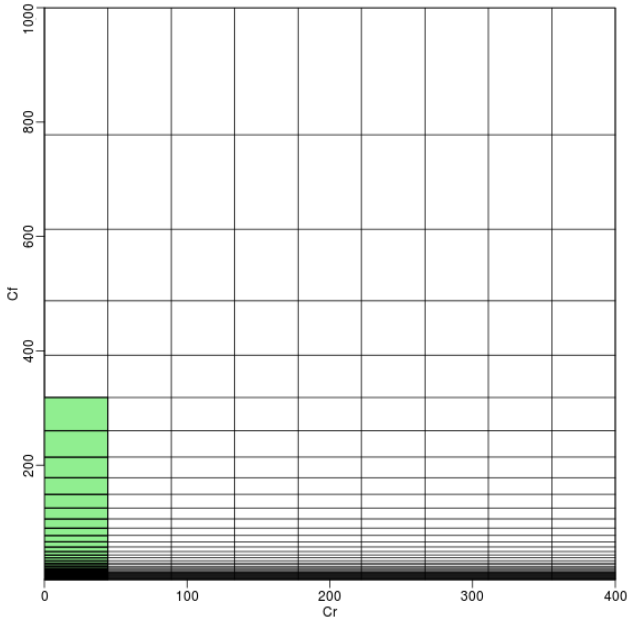

Fig. 4. Visualisation of a slice of the state space for the variables C_r and C_f in the Grimaud model. Green region represents states which belong to the attractor. The values of the remaining variables are fixed to $N_r \in [44.44,\ 66.66]$ and $C_{nit} \in [0,\ 0.111]$.

The attractor is spread on entire rectangular state space corresponding to the entire admissible space. In full dimensions, the actual attractor has a very complex shape and it covers less than 8% of the volume of this space.

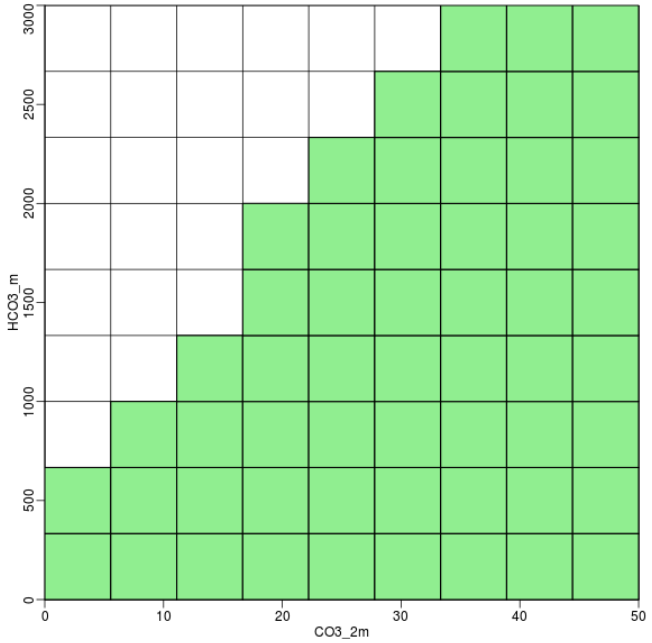

Fig. 5. Visualisation of a slice of state space for variables CO_3^{2-} and HCO_3^- in Müller model. Green regions represent states which belong to the attractor. The values of the rest of the variables are arbitrary except OH^-, which is in the range $[0.111,\ 0.222]$.

Plyusnina model. Since there are no unknown parameters in the model, we have run the attractor analysis for the particular parametric valuation resulting in a single attractor. However, the shape of the attractor is extremely complex to be effectively visualised.

The attractor is spread almost on the entire rectangular state space. However, the shape of the attractor is very complex and does not cover the entire state space, only approximately 47%.

V. Discussion

We have shown an application of our recently developed attractor detection method to several dynamical models describing biophysics of cyanobacteria. On the theoretical side, the main advantage of the method is the ability to detect attractors without precise knowledge of systems behaviour or even its parameters. On the practical side, the used implementation of the method relies on rectangular abstraction that approximates the dynamics of an ODE system in case it is non-linear. Combining both aspects gives us a unique fully automatised algorithm for attractor analysis that performs well on typical dynamical models used in biophysics.

It is worth noting that our algorithm adapts the known parallel algorithms [18] to the parametrised setting and adds the possibility to accelerate the computation if only the number of tSCCs is requested without the need to enumerate the attractors. In consequence, deploying it to high-performance platforms allows us to analyse complex multi-dimensional systems under non-trivial parameter uncertainty.

The case study conducted in this paper has covered a variety of non-linear models differing in dimension and number of unknown parameters. In case of well-developed models that are already accepted and used in the domain of cyanobacteria systems biology, the obtained results are in agreement with the expectations of the modellers. In case of incomplete models, the results make an interesting feedback to the modellers and thus make an important input for the model tuning and curation procedure.

References

[1] J. Barnat, N. Beneš, L. Brim, M. Demko, M. Hajnal, S. Pastva, and D. Šafránek, "Detecting attractors in biological models with uncertain parameters," in *CMSB 2017*, ser. LNBI, J. Feret and H. Koeppl, Eds., vol. 10545. Springer, 2017.

[2] D. Dudkowski, S. Jafari, T. Kapitaniak, N. V. Kuznetsov, G. A. Leonov, and A. Prasad, "Hidden attractors in dynamical systems," *Physics Reports*, vol. 637, pp. 1–50, 2016, hidden Attractors in Dynamical Systems.

[3] G. Batt, B. Yordanov, R. Weiss, and C. Belta, "Robustness analysis and tuning of synthetic gene networks," *Bioinformatics*, vol. 23, no. 18, pp. 2415–2422, 2007.

[4] P. J. Collins, L. C. Habets, J. H. van Schuppen, I. Černá, J. Fabriková, and D. Šafránek, "Abstraction of biochemical reaction systems on polytopes," *IFAC Proceedings Volumes*, vol. 44, no. 1, pp. 14 869–14 875, 2011.

[5] R. Grosu, G. Batt, F. H. Fenton, J. Glimm, C. L. Guernic, S. A. Smolka, and E. Bartocci, "From cardiac cells to genetic regulatory networks," in *CAV'11*, ser. LNCS, vol. 6806, 2011, pp. 396–411.

[6] D. Sullivan and R. Williams, "On the homology of attractors," *Topology*, vol. 15, no. 3, pp. 259–262, 1976.

[7] T. Chatain, S. Haar, L. Jezequel, L. Paulevé, and S. Schwoon, "Characterization of reachable attractors using petri net unfoldings," in *CMSB 2014*, ser. LNCS, P. Mendes, J. O. Dada, and K. Smallbone, Eds., vol. 8859. Springer, 2014, pp. 129–142.

[8] S.-M. Choo and K.-H. Cho, "An efficient algorithm for identifying primary phenotype attractors of a large-scale boolean network," *BMC Systems Biology*, vol. 10, no. 1, p. 95, 2016.

[9] W. Guo, G. Yang, W. Wu, L. He, and M. Sun, "A parallel attractor finding algorithm based on boolean satisfiability for genetic regulatory networks," *PLOS ONE*, vol. 9, no. 4, pp. 1–10, 2014.

[10] M. Demko, N. Beneš, L. Brim, S. Pastva, and D. Šafránek, "High-performance symbolic parameter synthesis of biological models: A case study," in *CMSB 2016*, ser. LNBI, E. Bartocci, P. Lio, and N. Paoletti, Eds., vol. 9859. Springer, 2016, pp. 82–97.

[11] G. Batt, R. B. Salah, and O. Maler, "On timed models of gene networks," in *Formal Modeling and Analysis of Timed Systems (FORMATS)*, ser. LNCS. Springer, 2007, pp. 38–52.

[12] N. Beneš, L. Brim, M. Demko, S. Pastva, and D. Šafránek, "Pithya: A parallel tool for parameter synthesis of piecewise multi-affine dynamical systems," in *CAV 2017*, ser. LNCS, R. Majumdar and V. Kunčak, Eds., vol. 10426. Springer, 2017, pp. 591–598.

[13] M. Troják, D. Šafránek, J. Hrabec, J. Šalagovič, F. Romanovská, and J. Červený, "E-cyanobacterium.org: A Web-based Platform for Systems Biology of Cyanobacteria," in *CMSB 2016*, ser. LNBI, vol. 9859. Springer, 2016, pp. 316–322.

[14] S. Hoops, S. Sahle, R. Gauges, C. Lee, J. Pahle, N. Simus, M. Singhal, L. Xu, P. Mendes, and U. Kummer, "COPASI Complex Pathway Simulator," *Bioinformatics*, vol. 22, no. 24, pp. 3067–3074, 2006.

[15] J. O. Dada, I. Spasić, N. W. Paton, and P. Mendes, "SBRML: a Markup Language for Associating Systems Biology Data with Models," *Bioinformatics*, vol. 26, no. 7, pp. 932–938, 2010.

[16] R. L. Clark, J. C. Cameron, T. W. Root, and B. F. Pfleger, "Insights into the Industrial Growth of Cyanobacteria from a Model of the Carbonconcentrating Mechanism," *AIChE Journal*, vol. 60, no. 4, pp. 1269–1277, 2014.

[17] G. M. Grimaud, S. Rabouille, A. Dron, A. Sciandra, and O. Bernard, "Modelling the Dynamics of Carbonnitrogen Metabolism in the Unicellular Diazotrophic Cyanobacterium Crocosphaera watsonii WH8501, under Variable Light Regimes," *Ecological Modelling*, vol. 291, pp. 121 – 133, 2014.

[18] J. Barnat, J. Chaloupka, and J. Van De Pol, "Distributed algorithms for SCC decomposition," *Journal of Logic and Computation*, vol. 21, no. 1, pp. 23–44, 2011.